IC/2000/170

the
abdus salam
international
centre
for theoretical
physics

united nations
educational, scientific
and cultural
organization

international atomic
energy agency

SHAPE ANALYSIS OF ISOSEISMALS BASED ON EMPIRICAL AND SYNTHETIC DATA

G. Molchan

T. Kronrod

and

G.F. Panza

32/05

preprint

IC/2000/170

United Nations Educational Scientific and Cultural Organization
and
International Atomic Energy Agency
THE ABDUS SALAM INTERNATIONAL CENTRE FOR THEORETICAL PHYSICS

SHAPE ANALYSIS OF ISOSEISMALS BASED ON EMPIRICAL AND SYNTHETIC DATA

G. Molchan[1], T. Kronrod,
International Institute of Earthquake Prediction Theory and Mathematical Geophysics, Russian Academy of Sciences, Warshavskoe sh., 79, k.2, Moscow 113556, Russian Federation
and
The Abdus Salam International Centre for Theoretical Physics, SAND Group, Trieste, Italy,

and

G.F. Panza
Department of Earth Sciences, University of Trieste, Trieste, Italy
and
The Abdus Salam International Centre for Theoretical Physics, SAND Group, Trieste, Italy.

MIRAMARE – TRIESTE
November 2000

[1]E-mail: molchan@mitp.ru; Tel. +007 (095) 110-7795; Fax: +007 (095) 310-7032

Abstract. We present an attempt to compare modeled ground motion acceleration fields with macroseismic observations. Two techniques for the representation of the observed intensities by isoseismals, a smoothing technique and one which visualizes the local uncertainty of an isoseismal, are tested with synthetic and observed data. We show how noise in the data and irregularities in the distribution of observation sites affect the resolution of the isoseismal's shape. In addition to "standard" elongated shapes, we identify cross-like patterns in the macroseismic observations for two Italian earthquakes of strike-slip type; similar patterns are displayed by the theoretical peak acceleration fields calculated assuming the point source models given in the literature.

1. INTRODUCTION

Macroseismic intensity, *I*, is a descriptive quantity characterizing the impact of seismic ground motion on people, built environments and landscapes. The scales for *I* bear the imprint of historical time and reflect the national construction practices prevailing in a country (Trifunac & Brady, 1975), nevertheless, there is an unflagging interest in macroseismic data, because these are indispensable to seismic risk assessment (see e.g. Keilis-Borok *et al.*, 1984, 1984a).

The macroseismic (MS) data for an earthquake consists of a set of "site-intensity" pairs termed Intensity Data Point (IDP) map. The data have two features, which impede their effective use:

— measurement sites form an irregular set of points that depends on the distribution of the population in the area;

— observed *I* values involve a "noise" component, which is due, for instance, to measurement errors and local inhomogeneities in the structure of the Earth's crust. The observed spatial variations of *I* over distances in the range from 20 to 40 km may be as large as 3 to 4 intensity units (see below). This is usually true for the recent data due to the higher site density and to the poorer preprocessing with respect to historical data.

Recent electronic publications (Boschi *et al.*, 1995, 1997; Monachesi & Stucchi, 1997) have made available IDP maps for Italian earthquakes, and have renewed the interest for some old problems connected with MS data:

— the automatic intensity data reduction or the objective generalization of IDP maps which help to lower the "noise" component and to represent the MS observations with continuous isolines (De Rubeis *et al.*, 1992; Tosi *et al.*, 1995);

— the use of MS data for refining and/or estimating the parameters of an earthquake source (Karnik, 1969; Shebalin, 1972; Zahradnik, 1989; Panza *et al.*, 1991; Johnston, 1996; Gasperini *et al.*, 1999; Sirovich and Pettenati, 1999).

These two problems are interrelated. For instance, the macroseismic estimates of magnitude, M, and depth, h, are based on the areas of the isoseismal zones $G_I = \{\text{intensity} \geq I\}$ and on the so-called mean MS field equation, i.e. a linear regression relation involving intensity, magnitude and logarithm of the hypocentral distance (Blake, 1941; Shebalin, 1959). This methodology is logically consistent with the generalization of an MS field obtained by smoothing the associated IDP map.

The situation becomes more complicated when one is concerned about the geometry of the seismic source or about the comparison between the MS data and theoretically predicted peak values of ground motion (Panza *et al.*, 1991). In such cases reliable inferences about the isoseismal shape are needed. These cannot always be drawn from a smoothed IDP map and one needs a visualization of the local isoseismal resolution. For such a purpose one can replace each isoline with a boundary zone of variable width, that reflects the uncertainty of the relevant isoseismal.

We consider two approaches for the generalization of IDP maps. One involves a smoothing procedure, which generalizes the local polynomial filtering used by De Rubeis *et al.* (1992) and Tosi *et al.* (1995). In our approach, the Modified Polynomial Filtering (MPF), the radius of the local filtering is variable and it is adapted to the local structure of the MS data, incorporating the discreteness of the intensity scale *I*.

The other approach, which we call the Diffused Boundary (DB) method, visualizes the uncertainty of isoseismals. This method essentially relies on the fact that *I* is a discrete quantity. This property of the MS data has nearly never been integrated in automated smoothing techniques applied to IDP maps.

Tests applied to real data demonstrate that the two methods are complementary when one has to decide about the shape of isoseismals.

2. SMOOTHING TECHNIQUES FOR IDP MAPS

2.1. Informal techniques

Hand techniques for smoothing IDP maps are not reproducible, but one can discuss the principles

on which they are based. Shebalin (2000) summarized the requirements on isoseismals as follows:

(a) isoseismal zones G_I must be simply-connected and embedded, expanding with increasing isoseismal rank I_0–I (*the monotonicity condition*);

(b) any isoseismal of level I is an external contour enclosing areas of reliably determined intensities I (the generally accepted *convention* to define an isoseismal);

(c) adjacent isoseismals are approximately similar (*similarity*);

(d) the curvature of an isoseismal must be as small as possible, and nonnegative (the *simplicity condition*, which gives an additional guarantee of smoothness for the isoseismals);

(e) the number of sites with $I \geq J$ outside a zone G_J is approximately equal to that of sites with $I < J$ in the G_J zone itself (*equality of the errors of the two kinds*);

(f) consecutive isoseismals along an azimuth must be neither too close nor too far from each other (*a mild control of the mean field model*).

Contemporary data show that the boundary between two adjacent intensities may be rather diffused. For this reason requirement (e) about the equality of the errors of the two kinds may contradict the definition of isoseismals (convention (b)). In fact, let the MS field be isotropic and the observations with I-1 and I be well mixed in the annulus $r_1 < r < r_2$. If we assume that there are no points with I-1 inside the circle $r \leq r_1$ and no points with I outside the circle $r = r_2$, then, according to (b), the circular line $r = r_2$ has to separate the intensities I-1 and I. As a result all the observations of level I but not all of level I-1 will be correctly identified.

The monotonicity, similarity and smoothness properties unfortunately can be tested using only some instrumental analogues of MS intensity: peak values of the wave field in terms of acceleration, velocity or displacement. Panza *et al.* (1991) use the modal summation technique to model the wave field produced by an instantaneous seismic point source in a plane-stratified Earth. These computations point to complexities in the structure of the modeled ground motion fields in

the zone near to the epicenter (within 200 km). In particular, one may have 2 to 4-lobe isoseismals, violations of the similarity condition and of the other requirements listed above. The reasons given in Burger *et al.* (1987) support the local violations of monotonicity of the peak acceleration field at distances of 60-120 km from the source, due to the competitive effect of direct and postcritically reflected S waves from the Moho.

Taken as a whole, Shebalin (2000) conditions are based on the experience gained when working with small data sets and they aim at the simplest problems in MS data interpretation, such as the determination of the earthquake scalar seismic moment, source location and azimuth. That is why they reduce the isoseismal shape to a simple oval, unless the data definitely states to the contrary.

2.2. Filtering techniques

To smooth IDP maps De Rubeis *et al.* (1992) and Tosi *et al.* (1995) applied a local polynomial filtering. The method is based on the assumption that the macroseismic field can be well fitted locally with a polynomial of degree two, $P_2(g)$. The fit to the field at a given point g_0 is found by considering a circle $B(g_0,R)$ centered at g_0 and having radius R. Let $P_2(g)$ approximate the I-data in $B(g_0,R)$ with minimal squared error. Then the polynomial at the center of the circle is taken to be the desired estimate of the field $\hat{I}(g_0)$ at g_0. Following requirement (b) in Section 2.1, the isoline $\hat{I}(g)=I-\Delta I/2$ can be regarded as the isoline of the macroseismic field relevant to level I, ΔI being the discretization interval of the intensity scale. It should be borne in mind, when choosing the smoothing parameter R, that the real density of the observations is generally non-uniform.

Constant value of R. De Rubeis *et al.* (1992) used a constant value of R. In this case the residual noise component in a smoothed MS field may be subject to great lateral variability, the associated variance being obviously greater in areas of lower observation site density, because of the fewer data in the averaging circle. The deterministic component of the MS field varies rapidly

in the epicentral zone and more slowly at the periphery. According to Shebalin (1959), the mean distance between isolines of levels I and I-1 increases with I decreasing in a geometric progression with the coefficient $k \approx 2$, if the epicentral distances are within 300 km. For this reason the choice of large R is generally neutral to the smoothing of the deterministic part of the MS field at the periphery, but can significantly affect the isoseismal shapes in the near zone.

In many IDP maps of Italian earthquakes we have noticed that the density of the I-points appreciably decreases from the epicenter to the periphery (*effect A*). We see it on the three of four Italian earthquakes, considered in this paper (Fig.1). One possible explanation of the effect A may be the nonuniform inspection, which is more detailed at the epicenter, where the MS effect is high, and much less at the periphery, owing to both economic reasons and the *a priori* slow variability of the MS field. When R is constant, the effect A favors an increase of the residual noise component at the periphery of the MS field.

The shortcoming of a constant R has been overcome in a later work by Tosi *et al.* (1995), where the smoothing cell remains standard, but it is defined in polar coordinates, centered at the epicenter of the event. For this reason the actual linear size of the smoothing area is decreasing toward the center. Nevertheless, the density of observations may be rather irregular, so that the smoothing cells remain, generally speaking, nonuniform with respect to the number of measurement sites. One natural way out of this difficulty is to use areas $B(g_0, R)$ of variable radius by adapting them to the geometry of the measurement sites around g_0.

Non-constant R value (Modified Polynomial Filtering, MPF). For every point g_0 the radius R is chosen within a specified set $\{R_i\}$ with the condition $R<L/3$, where 2L is the diameter of the circle enclosing the entire set of all measurement sites. Taking values of R_i in increasing order, we can find the first area $B(g_0, R)$ that contains at least n_p observation sites and in which the number of different integer intensity values is not below a threshold $n_I>1$.

When the threshold n_p has been overcome, small values of n_I are practically negligible in the

epicentral zone because of the large variations in the deterministic component of the MS field. For this reason the radius R will be small near the epicenter. On the other hand it is natural to use a larger averaging radius at the periphery. Suppose we have little noise in the MS data. Then using n_I=2 we will expand the averaging area until it reaches the boundary of the adjacent intensity. Since the intensity scale is discrete and the noise is small, the expansion will not distort our estimate near g_0 of the trend of MS field, which is almost constant in the considered case.

The set $\{R_i\}$ has been used as {id, i=1,2,...}, where d is the typical size of the highest (lowest rank) isoseismal, d≅10–20 km. The threshold n_p is taken equal to 6m. The two-dimensional polynomial P_2 has 6 parameters; therefore "m" is the average number of measurements per parameter. Usually we set m=2–3, because larger values of "m" increase the averaging area, leading to poorer isoseismal resolution. The poor resolution controls the choice of the degree, k, of the smoothing polynomial, P_k, as well. In fact, in general P_k has (k+1)(k+2)/2 parameters. Therefore, if k>2 and the number of *I*-points in $B(g_0, R)$ is small, the estimates of the polynomial parameters will be not stable. On the other hand, however, the degree k, should be greater than 1, because the boundary between adjacent intensities is curved. For data involving moderate (large) noise we use for the threshold n_I the values 2÷3 (3÷4).

The procedure gains in stability when the averaging areas strongly overlap, as in the case of small spacing $|\Delta g_0|$ of the grid $\{g_0\}$, whose knots are the centers of the regions $B(g_0,R)$. In actual practice one has $|\Delta g_0|$=3÷5 km. The obvious bias in the estimates of the local trend of P_2 occurs at the periphery of an IDP map when the observation sites, falling into the averaging area $B(g_0, R)$, are seen from g_0 at an angle $\varphi<180^\circ$. Then g_0 is a point where the field $I(g)$ has to be extrapolated, i.e., it is a location where the fit $P_2(g)$ is not constrained by observations. An additional threshold for the angle φ, $\varphi\geq\varphi_0$, is then used to exclude such effects. This either increases the averaging radius or excludes the point from consideration. In our examples $\varphi_0=200^0$.

Fig. 2a gives an example of the spatial distribution of R(g) for the 1997 Colfiorito earthquake (Central Italy). It shows that R is automatically increasing from the epicenter toward the periphery. In addition, Fig. 2b shows the number, $\nu(g)$, of the intensity measurements in each area B(g, R). This quantity has weak fluctuations along the isolines and at the periphery, e.g. $\nu \cong 20$, $R \cong 20$ km along the isoline of the third rank, I=VI. Some perturbations of $\nu(g)$ at the periphery are explained by the boundary effect in the filtering, which is controlled by the parameter φ_0.

Overall, the merit of formalized filtering techniques is that they are reproducible and do not involve *a priori* restrictions on the shape and connectedness of the isoseismals. The polynomial filtering partly suppresses the noise and the local components in the observations and does not distort the polynomial trend of degree two when there is no noise. However the interpretation of the shape of the isoseismals remains problematical, owing to possible smoothing-out of details. The use of filtering techniques is natural with respect to continuous fields, but the intensity takes integer values, in our case in the range from III to IX, and there may be only 2 or 3 different values in the vicinity of the boundary between two intensities. The effect of the discreteness of the I scale on the isoseismal's shapes of a smoothed IDP map has not yet been investigated.

3. VISUALIZATION OF THE UNCERTAINTY IN THE ISOSEISMALS

3.1. The Diffused Boundary (DB) method.

The analysis of the shape of an isoseismal requires the visualization of its local uncertainty. Speaking in terms of mathematical statistics, the problem can be interpreted as the passage from the point estimation of an isoline to the interval estimation. The local thickness or uncertainty of an isoline must depend on the local geometry of the measurement sites and on the noise component present in the data. The solution we propose in this section essentially relies on the fact that the intensity scale is discrete. We assume that the isoseismal zones G_I are simply connected and monotonic. The connectedness assumption is not absolutely indispensable, as we shall see.

1- D case. To explain the principles of the DB concept let us start from the case of 1-D MS

data. Isoseismals on a line make a set of embedded intervals with intensity $\geq I$ that are increasing with decreasing I. For a given intensity level, we must separate points of two types on the line: "+" with intensity $\geq I$ and "0" with intensity $< I$ (Fig. 3a). When the observations are error-free, a cluster of pluses lies between two clusters of zeroes. (As cluster on a line we mean a nonempty sequence of identical characters that cannot be expanded without adding a different character.) The true boundary of level I is covered by two intervals, Δ_- and Δ_+, that separate the clusters and supply all available information on the boundary uncertainty, no smoothing techniques are being able to improve the boundary between "+" and "0".

When MS observations contain noise, the pattern is more complex: some pluses percolate into the zeroes zone and conversely (see Fig. 3b). For simplicity Fig. 3b presents only the right semi-axis which starts from the barycenter of the pluses. In view of possible errors in the observations we allow some pluses, up to the amount $\varepsilon\%$ of the total number of pluses on the semi-axis, to be considered as erroneous. Because of the convention (b) about isoseismals we are primarily interested in the outer boundary of pluses. For this reason the first candidates to be classified as erroneous will be those pluses farthest from the center. Under these new conditions the interval, say Δ_+, is specified uniquely by the following requirements. It is the interval (a, b) which separates the pluses cluster contained in the interval $[a', a]$ and the zeroes cluster contained in the interval $[b, b']$ (see Fig.3b). We assume that $I(\infty)=0$, so that the point "∞" always belongs to the set of measurements, and require that in the interval (a,∞) the number of pluses is $\leq\varepsilon\%$ of all pluses on the semiaxis, and $>\varepsilon\%$ in the interval $[a',\infty)$.

Let us consider the following example (Fig. 3b). Two pluses, marked with arrows in Fig. 3b, of the twelve could be removed at the level $\varepsilon=20\%$. We remove only one plus (the rightmost one) because the other belongs to the cluster of 3 pluses and can be removed only together with the cluster. The removal of the cluster (3 pluses) violates our rule on the ε-threshold since

(1+3)/12>20%. The resulting boundary Δ_+ is shown in Fig. 3b. Thus a distant cluster of pluses cannot be classified as erroneous, unless it is comparatively small, and as a rule it is preserved as a whole, when its size is an evidence that the observed intensity is a genuine effect.

2-D case. The local uncertainty of an isoseismal in the 2-D case can be obtained by inspection of the *I*-points in the vicinity of each straight line traced on the MS field. The traces of G_I on any cross-section of the MS field will inherit the connectedness and monotonicity of the MS field, therefore to find an intensity boundary we may use the criteria defined in the 1-D case.

Let us consider a strip across an IDP map. The strip is specified by the distance, r, of its axis from the epicenter, by the direction, φ, of that axis, and by the width, H, playing the role of a smoothing parameter. Projecting all points lying in this strip onto its major axis, we get a 1-D variant of the problem. Fig. (3a, 3b) now illustrate the decisions regarding the boundary between the observations that fall into the strip. Since the strip is two-dimensional, we consider rectangles of size H/2 x $\Delta_\pm$ (see Fig. 3a, 3b) as the local boundary of level *I* along the straight line (r, φ). This rectangle is called the *Local Diffused Boundary* (LDB), and its indicator function, having the values 1 for points of the rectangle and 0 otherwise, will be termed *LDB-function.*

Evidently, a single LDB can be unstable due to the strong dependence on the choice of ε. But sorting out all possible sections (r, φ) of the IDP map, we obtain a 2-D family of local boundaries, the *Diffused Boundary* (DB), for a given intensity. The new object, DB, is more stable and supplies information on the uncertainty of G_I at any point of the space, in any direction, while a number of overlapping LDB elements in each point can be interpreted as a local measure of the reliability for the diffused boundary.

The visualization of DB can be made with two different methods. With one method only LDB axes are plotted in the MS field with some discretization of (r, φ). The emerging picture looks like a thorny "hedgehog". This visualization will therefore be called a *"thorny" diffused boundary*. With the other method we take into account the fraction of overlapping LDB elements

in each point. To do this we sum all LDB-functions and get a *DB-function* with a maximum M. The area where the DB-function exceeds the level pM, 0<p<1 is considered to be the *p-diffused boundary* of G_I.

When an isoseismal G_I is not convex or not simply connected, the DB-function can be underestimated for the boundary points of G_I which are internal to the convex hull of G_I. The reason is that we take into consideration only two (the left- and right-most) boundary points of G_I in any cross-section of the MS observations.

Threshold p. It is advisable to consider idealized situations in order to choose the threshold p. Let us assume that we have noise-free observations, the observation sites with intensity $\geq I$ filling the entire circle of radius R_1, B(O,R_1), and those with intensity $<I$ filling a circle of radius $R_2>R_1$ at the same center, O. We also assume that there are no observations in the annulus $R_1<r<R_2$. If the strip width is H=0 then the DB-function is equal to the angle $\varphi(g)$ at which the area B(O, R_1) is seen from g; $\varphi(g)\equiv 0$ for g out of the annulus. Hence the threshold p is connected with the distance $r \geq R_1$ by the relation

$$p(r) = \begin{cases} 2\pi^{-1} \arcsin(R_1 / r), & R_1 \leq r \leq R_2 \\ 0, & r > R_2 \end{cases}$$

i.e., p=1, $^1/_2$, and $^1/_3$ for $r = R_1, \sqrt{2}R_1$, and $2R_1$, respectively if $r<R_2$.

Frequently MS data are interrupted by a coastline. The theoretical analysis of the DB in this case is important for the correct interpretation of DB peculiarities of lobe-like type. As a model let us consider the previous example and eliminate all observations with intensity $<I$ from the half-plane $x>x_0$ where $R_1<x_0<R_2$ (see Fig.3c). If H=0 the DB-function has the same geometric meaning as above. Therefore when $R_2>R_1/\sin(\pi p/2)= R_1^*$ the p-diffused boundary of G_I is identical to the annulus $R_1 \leq r< R_1^*$. Otherwise (see Fig. 3c) the p-diffused boundary consists of the annulus $\{R_1< r<R_2\}$ and of a local outgrowth on it directed toward the axis x within

$R_2 < x < \min(R_1^*, R_2^*)$, where

$$R_2^* = R_2 \sin(\pi p/2 + \gamma)/\sin(\pi p/2),\ \gamma = \arccos(x_0/R_2).$$

In the real cases $R_2 < (1.5 \div 2)R_1$ and therefore the DB zone contains the entire annulus if $p = 1/3 - 1/2$; for $R_2 \le \sqrt{2}R_1$ and $p = 1/2$ the R_2^* value is $\sqrt{2}R_1$.

The main parameters of the DB method. To analyze MS data for Italy we use the following values of the main parameters: ε=5–15%, strip width H=20–40 km, threshold $p = 1/3 - 1/2$. The other parameters are connected with the discretization of the family of strips: (r, φ) are discretized with steps Δr =0.1 H and $\Delta\varphi = 5^\circ$, respectively.

Many recommendations about hand treatment of IDP maps contain the advice to map the local reliability of the isoseismals (see e.g. Shebalin, 2000). The diffused boundary of G_I is derived by inspection and by incorporation of the uncertainty in the isoseismals at each point and in each direction. For this reason the proposed version of the boundary of G_I, as a stripe of varying thickness, can be regarded as one of the possibilities for the visualization of the uncertainty in the isoseismals.

Colfiorito earthquake, 26.IX.1997, Mw =6.0, I_0=IX, IDP map by GNDT (1997), number of I-points n_{obs}=362.

We have illustrated the filtering technique MPF (see Fig.2) using this event, which is the largest earthquake in Italy in the recent past with a good set of MS data. In fact, the Italy catalog NT4.1 by Camassi and Stucchi (1997) contains only 10 events, for the period 1900-1980, with $n_{obs} \ge 300$. The main event has been preceded by a foreshock (M_w=5.7 about 8 hours before) with a similar focal mechanism (normal faulting) but different location, nevertheless the intensity data of the Colfiorito event, for $I \ge$V, are low-noise and relatively dense in space. As a result the residuals between the observed and the smoothed values of I are, in general, within 0.5, over the entire area considered. Figure 4 shows that the isoseismals derived by MPF and DB methods are fairly

well consistent. Both methods indicate a possible lack of connectedness in the I=VI isoseismal. On the whole, Fig. 4 can be regarded as an illustration of the isoseismal resolution based on intensity data of good quality. At the same time, Fig. 4 is not suitable for an interpretation in terms of source and site effects owing to the superposition of the effects of two large shocks [Tosi et al., 1999].

4. EMPIRICAL AND SYNTHETIC ISOSEISMALS: EXAMPLES OF COMPARISON

The developed technique can be applied to the comparison between the empirical and the synthetic isoseismals. To this end we choose three Italian earthquakes of strike-slip type because their synthetic isoseismals show non-trivial cross-like shapes instead of the "standard" elongated shapes.

The synthetic isoseismals are defined as follows. We generate the synthetic seismograms by mode summation (Panza, 1985; Panza & Suhadolc, 1987; Florsch *et al.*, 1991) at frequencies below 1 Hz. These calculations are based on a plane-stratified schematic crustal model for Italy (Costa *et al.*, 1993) and on the instantaneous point source approximation taken from the literature, scaled accordingly with Gusev (1983) source spectra, as reported by Aki (1987). The synthetic isoseismals are defined in terms of peak values of acceleration a_p, velocity v_p or displacement d_p. For example, the a_p-isoseismal of the intensity level I_a is the area $\{a_p < a_p\ (I_a)\}$ where

$$\log a_p(I_a)\ [\mathrm{cm/s^2}] = b_0 + b_1(I_a - 6). \qquad (1)$$

The value b_1=0.3 that corresponds to the relation $a_p(I_a\text{-}1)/\ a_p(I_a)$=2 is usually used for the classification of MS effect and not contradicted by the numerous empirical relations (see Shteinberg *et al.*, 1993 and references therein); the gauge coefficient $b_0=\log a_p(I_a=6)$=0.47 was derived for Italian earthquakes by Panza *et al.* (1997, Table 1, I=VI).

The main difficulty, that arises in such approach to the isoseismal comparison problem, is that the intensity data usually are the result of the cumulative effects of a sequence of events that includes the mainshock and its fore- and aftershocks. Additional factors affecting the isoseismal

size and shape are:

— the local soil effect or more generally the local inhomogeneites in the Earth structure which *a priori* are unknown;

— the discretization given by (1); Panza *et al.* (1997) found that the average coefficient b_0 depends on the choice of the version of the Italian catalogs and this leads to the shift in the intensity I_a by one unit; in addition, the parameter, b_0, depends on the quality factor, Q, which is varying with the crust;

— the earthquake depth; it is usually a poorly defined parameter, if the wave field, near the fault zone of large shallow earthquake, is modeled with a point source; therefore the isoseismals of the first and/or second rank can be not suitable for the comparison, due to the point approximation of the source.

To control the depth effect we use the condition $D(I)>3l$, where D is the average hypocentral distance of the intensity I and l is the linear size of the source; following Gasperini *et al.* (1999) we assume:

$$\log l\,[\mathrm{km}] \cong 0.6\,M_w - 2.3. \qquad (2)$$

The isoseismals of high rank for Italy are often unsuitable as well since their boundaries are not closed. Thus the choice of the isoseismals for the shape analysis, in general, is limited to one or two intensity degree for each earthquake.

Potenza earthquake (Southern Italy), 5.V.1990, M_w=5.8, I_0=7, I_{max}=VII-VIII, IDP map by BMS (1990).

The MS data for the Potenza earthquake are unusual due to the high density of IDP (Fig. 5a, Fig.1), n_{obs}=1372, and the exceptionally high "noise" in the data. For example, the spatial variation in intensity is occasionally as high as 4 units over distances of about 40 km. This can be seen in Fig. 6 which gives a subdivision of the relevant space into rectangular cells in polar coordinates and the histograms of the observed I in three representative cells. This is also shown by the

residuals δI between the observed and the filtered values of I. They are very large $\delta I \in (-3, 3)$ and vary over space (see Fig. 5a). The "noise" is not the result of cumulative effects of the aftershocks sequence because they are concentrated near the main shock (see Fig. 5b) and the strongest aftershock has a local magnitude M_L=4.7.

Of the two sources of noise, namely, the spatial distribution of the observation points and the noise in I, the latter becomes the most important, when the measurement sites are dense. Therefore from *a priori* considerations the polynomial filtering is preferable in the present example. The MPF method focuses on local smoothing of the noise, while the DB method incorporates observations contained in complete cross-sections of an IDP map. Figure 5 shows that the two methods yield very different results for the rank 1 isoseismal (I=VI), but they are moderately consistent for the rank 2 isoseismal, the other isoseismals being non-closed.

We calculate ground motion fields for a scaled point source with the parameters:

strike 184°, dip 73°, rake 13°, focal depth 10 km (CMT).

The theoretical a_p-isoseismals, shown in Fig. 7a as thin continuous lines, have a cross-like shape and are not consistent with the isolines of the IDP map shown in Fig.5. Since the noise is large, to see what part it played in producing the inconsistency, we add noise to the theoretical a_p values computed in the real observation sites.

The noise varies over the area. For this reason we use the analysis of the spatial variation of I as shown in Fig. 6. A frequency histogram of the observed I is calculated for each elementary area. Each histogram is centered at the median and it is assumed to represent the error distribution in the elementary area concerned.

Figure 7 shows the results of the reconstruction of the a_p field when dealing with noisy synthetic data. The DB method (Fig. 7b) gives a good reconstruction of the cross-like structure of the I_a=VII isoseismal, while the MPF method reconstructs the I_a=VI and I_a=V isoseismals. The DB method does not work for the $I_a \leq$VI isoseismals because of the presence of the quadrangular

large noise anomaly, indicated in Fig. 5a by a bold arrow.

It thus appears that even if the noise level is high the availability of a dense set of observation sites allowed us to reconstruct the theoretical a_p field (thin line in Fig.7a). The discrepancy between the thick lines in Fig. 5a and 7a suggest that the assumption made about the source or/and the crust model is not adequate to describe the MS data for the case under consideration.

Alpago earthquake (Northern Italy), 18.X.1936, M_L=5.8, I_0=IX, IDP map by Boschi *et al.* (1995, 1997), and by Monachesi and Stucchi (1997), n_{obs}=292.

This earthquake has the following source parameters:

strike 193±3°, dip 61±1°, rake 7.5±5.5°, focal depth h=18 km (Costa *et al.*, 1993).

From (2) the linear size of the source can be estimated as $l \cong 11$ km. (We assume that $M_L \approx M_w$ in the range $M_L \in (4, 6.3)$, according to the (M_L, M_w) regression by Giardini *et al.* (1997) for the Mediterranean region.) Therefore the critical epicenter distance for the shape analysis is $\Delta = ((3l)^2 - h^2)^{1/2} \cong 30$ km. Judging from Fig.8, where the isoseismals obtained by the MPF method are presented, the suitable isoseismal for the analysis is the area of third rank (I=VI). This isoseismal is triple-connected and the dominant part of this area has a cross-like shape (see Fig. 8a).

The synthetic isoseismals have a well delineated cross-like shape, independent of the focal depth h in the range 7–20 km, which was used in our calculations (see, for example, Fig. 8b for h=18 km), and the area A of the a_p-isoseismal of level I_a=VI is a weak function of h:

h:	9	15	21
log A [km^2]	3.8	3.6	3.7

These values are close to the empirical estimate $\hat{A}$: $\log \hat{A}$=3.9, obtained by the MPF method.

Also Figure 8b shows the reconstruction of the isoseismal of I_a=VI, obtained for the synthetic a_p field calculated at the actual sites where the MS data have been observed. In converting a_p to I using (1) we preserve the same accuracy ($^1/_2$ or 1 unit of I) as in each real intensity-point obser-

vation. Judging from Figures 8a and 8b the dominant parts of the synthetic and empirical isoseismals of level I=VI are very similar in shape. The dominant part of the isoseismal area I≥VI, G', is clearly divided into two parts by a straight line (AA' in Fig. 8a). If Fig. 8a is compared to the relief, the northeastern part of G' lies within a mountain landscape, while the southwestern one is on a plain covered by Quaternary deposits. Each part contains two lobes of G' that give a total cross-like shape to G'. This circumstance tells that there is no relevant influence of the relief on the dominant part of the isoseismal I=VI.

Let us now consider the two secondary parts of the empirical isoseismal for I =VI (VI-A and VI-B in Fig. 8a). Each of them is characterized by the value $\Delta I = I - I'$, where I' is the intensity level for the surrounding area; in our case ΔI=+1. The largest secondary part (VI-A, Fig. 8a) occupies a portion of the NE Po valley and it is natural to assume that the value ΔI =+1 is caused by local soil conditions.

To test this hypothesis we consider the relevant Italian earthquakes, which occurred after 1456, with well-defined (n_{obs}≥100 for the historical events) and multi-connected isoseismals. The number of such events, including the Alpago event, is 11 and their space distribution is given in the insert of Fig. 9. This figure gives a synoptic picture of the secondary parts ("islands") of the multi-connected isoseismals for all these earthquakes. For all isoseismal parts ΔI≥+1, with the exception of isoseismal 4a, where ΔI=-1.

As can be seen, half of the VI-A area (Fig. 9), roughly coinciding with Euganei hills and Berici mountain, is covered by secondary parts of isoseismals of other earthquakes with the same intensity effect: ΔI=+1. The other part of VI-A area is extremely unstable and depends on a single measurement site with the anomalous value I=VIII (see in Fig.9 the bold point in the VI-A area). In the vicinity of the anomalous site, which is not reported in the Monachesi *et al.* (1997) data base, I≤VI. If the anomalous point is eliminated, the VI-A area reduces to the small area VI-C (in

Fig. 9), adjacent to the Euganei hills. Thus we can conclude that the synthetic model of the isoseismal I=VI is in good agreement with the IDP-map. The two secondary parts of the observed isoseismal (VI-A, VI-B, Fig. 8a) result from local inhomogeneities in the earth's structure, from the geometry of the measurement points, and from gross errors in the observations.

Irpinia earthquake (Southern Italy), 21.09.1962, M_L=6.1, I_0=IX, IDP map by Boschi *et al.* (1995, 1997) and by Monachesi and Stucchi (1997), n_{obs}=221.

The results of the generalization of the third rank isoseismal (I=VI) using the two methods are displayed in Figs. 10a and 10b. The DB method delineates well the cross-like isoseismal shape and when the semi-infinite LDB zones related to the coastline are removed, the cross-like structure becomes even more pronounced. At the same time this structure is not resolved in the set of isolines derived by the MPF method, with the possible exception of isoline I=VI. The last isoline is compatible with the diffused boundary but we get more information about the shape considering in Fig. 10b not one but the whole ensemble of reasonable versions of isoseismal I=VI, consistent with the MS data. About the relief effect on the shape of the I=VI isoseismal, our conclusion is practically identical with that reached in the previous example. The two well-expressed lobes in the north of G_{VI} (see Fig. 10a and Fig. 10b) belong to two different morphostructural zones, the left lobe lying within a mountain country, while the right lobe belongs to the Apulian peneplain, covered by Quaternary deposits. In the southern part of the G_{VI} zone the relief effect on the isoseismal shape cannot be assessed due to the few observations and to the presence of the coastline.

The 1962 Irpinia earthquake is a multiple event consisting of a strong foreshock, M_L=5.9, of a mainshock, M_L=6.1, and of a moderate aftershock, M_L=4.5 (Di Filippo & Peronaci, 1963). The first two events are separated by a 10 minute interval and have a very similar epicenter, therefore can be equally responsible for the MS effect. According to Gasparini *et al.* (1985) only the foreshock is a strike-slip event:

foreshock FPS: strike=32°, dip=65°, rake = 11°

mainshock FPS: strike=314°, dip=70°, rake =241°

We take for the depth the values $h_{for}=h_{main}=8$ km given by Westaway (1987). Again, the a_p-isoseismal area for I=VI is a weak function of the focal depth. For example, in the case of the mainshock we have the following relation:

h	8	16	24	32
log A [km^2]	4.1	4.1	3.7	3.9

For focal depths in the range from 8 to 20 km the shape of the a_p-isoseismal I=VI is elongated for the mainshock and it is cross-like for the foreshock. The case with h=8 km is shown in Fig. 11. Comparing Figures 10 and 11 we may conclude that the shape of the empirical isoseismal I=VI (Fig. 10b) is in good agreement with the shape of the theoretical one for the foreshock (Fig.11a) but not for the mainshock (Fig.11b). The foreshock and mainshock have magnitudes 6.0±0.1, therefore we repeat our calculations assuming M=6.0 for both events and we compute their cumulative effect, defined as the maximum of the a_p-values caused by the two events. In such a way we obtain the new picture shown in Fig. 11c, compatible with Fig. 10b.

5. CONCLUSION

This paper deals with the problem of the reconstruction of the isoseismal shape, and an original technique has been developed for this purpose. Since the problem is difficult, we attacked the issue (probably for the first time) from two sides at once: generalization of MS data (discrete) to isoseismals (continuous), and modeling. The database of MS data like the one available now for Italy, the synthetic isoseismal modeling and the technique developed here provide a good basis for a systematic analysis of the relation between MS observations and source geometry.

In the assumption that the observed MS intensities always involve noise, we reduce the noise component with a modified polynomial filtering technique, which controls the local maximum error. Following the principle "the IDP map is unique, while the number of isoseismals that

is compatible with the map is infinite", in order to visualize the uncertainty of the isoseismals we have developed the DB method. The method is suitable for the analysis of isoseismals of rank>1 and it is used to visualize the whole ensemble of reasonable versions of isoseismal consistent with the MS data. We are unaware of approaches like the one proposed here, although the problem of visualizing the isoseismal's uncertainty has been debated for a long time.

We show how the shape analysis of isoseismals may significantly benefit from synthetic modeling of ground motion. The theoretical modeling of ground motion and the simulation of the noise in IDP synthetic maps are independent sources for the delineation of the isoseismal shape and for the analysis of the effects of noise and of site geometry. Unfortunately, the used model and its parameters are inexact and the interconnection between intensity and acceleration remains open to discussion. Taking into account that the MS data are affected by noise, site effect and space irregularity of observations, it is hardly justifiable to expect an exact coincidence between the shape of empirical and synthetic isoseismals. Therefore the results reported here for some Italian earthquakes should be regarded as the successes achieved by the joint use of the MS data processing procedure, developed in this paper, and the ground motion modeling with synthetic seismograms. For two strike-slip events we have found a cross-like pattern both in the MS and in the synthetic data, and this contradicts the conventional recommendations for the generalization of MS data, that usually advise the use of oval shapes. Finally, particularly important for engineering purposes, we show examples of the perspectives offered by the analysis of the multi-connected isoseismals to reveal site effects.

ACKNOWLEDGEMENTS.

We are grateful to V. Ez, A. Lander, A. Nikonov and V. De Rubeis for useful comments. This work is supported by grants: ISTC (project 1293-99), NATO SfP 972266, USNSF: EAR 9804859, the Russian Foundation for Basic Research (00-05-64097) and by Italian MURST and CNR.

REFERENCES

Aki, K., Strong Motion Seismology. In: Strong Ground Motion in Seismology (Eds. M.O.Erdik and M.N.Toksöz) (D.Reidel Publ., 1987) pp. 3-39.

Blake, A. (1941), On The Estimation of Focal Depth from Macroseismic Data, Bull. Seismol. Soc. Am., **31**:3, 225-231.

BMS: Bolletino Macrosismico, 1990. Instituto Nazionale di Geofisica, Unita Operativa Geodinamica, Roma.

Boschi, E., Ferrari, G., Gasperini, P., Guidoboni, E., Smriglio, G. and Valensise, G., Catalogo dei Forti Terremoti in Italia dal 461 a.C. al 1980 (ING-SGA, Bologna 1995).

Boschi, E., Guidoboni, E., Ferrari, G., Valensise, G. and Gasperini, P., Catalogo dei Forti Terremoti in Italia dal 461 a.C. al 1990. (ING-SGA, Bologna 1997).

Burger, R.W., Somerville, P.G., Barker, J.S., Herrmann, R.B. and Helmberger, D.V. (1987), The Effect of Crustal Structure on Strong Ground Motion Attenuation Relations in Eastern North America. Bull. Seismol. Soc. Am., 77, 420-439.

Camassi, R. and Stucchi, M. (1997), NT4.1, un Catalogo Parametrico di Terremoti di Area Italiana al di Sopra della Soglia del Danno: a Parametric Catalogue of Damaging Earthquakes in the Italian Area. Web site: http://emidius.itim.mi.cnr.it/NT/home.html

CMT: Harvard Centroid Moment Tensor Database, Harvard Seismology: CMT Search Results. Web site: http://www.seismology.harvard.edu

Costa, G., Panza, G.F., Suhadolc, P. and Vaccari, F. (1993), Zoning of the Italian Territory in Terms of Expected Peak Ground Acceleration Derived from Complete Synthetic Seismograms. J. Appl. Geophysics, 30, 149-160.

De Rubeis, V., Gasparini, C. and Tosi, P. (1992), Determination of the Macroseismic Field by Means of Trend and Multivariate Analysis of Questionnaire Data, Bull. Seismol. Soc. Am., 82, 1206-1222.

Di Filippo, D. and Peronaci, F. (1963), Indagine Preliminare della Natura Fisica del Fenomeno che ha Originato il Periodo Sismici Irpinio dell'Agosto 1962, Ann. Geofis, 16:4, 625-643 (in Italian)

Florsch, N., Föh, D., Suhadolc, P. and Panza, G. (1991), Complete Synthetic Seismograms for High-frequency Multimode Love Waves, Pure Appl. Geophys., 136: 529-560.

GNDT (1997), Earthquakes of September and October 1997 in Umbria-Marche (Central Italy), 1997. Web site: emidius.itim.mi.cnr.it/GNDT/T19970926-eng/home.html

Gasparini, C., Iannaccone, G. and Scarpa, R. (1985), Fault-plane Solutions and Seismicity of the Italian Peninsula, Tectonophysics, 117, 59-78.

Gasperini, P., Bernardini, F., Valensise, G. and Boschi, E. (1999), Defining Seismogenic Sources from Historical Earthquake Felt Reports, Bull. Seism. Soc. Am., 89:1, 94-110.

Giardini, D., Donato, M. and Boschi, E. (1997), Calibration of Magnitude Scales for Earthquakes of the Mediterranean, J. of Seismology, 1, 161-180.

Gusev, A.A. (1983), Descriptive Statistical Model of Earthquake Source Radiation and its Application to an Estimation of Short-period Strong Motion, Geophys. J.R. Astr. Soc, 74, 787-808.

Johnston, A. C. (1996), Seismic Moment Assessment of Earthquakes in Stable Continental Regions –II. Historical Seismicity. Geophys. J. Int., 129, 639-678.

Karnik, V., Seismicity of the European Area, Part 1. (Reid Publishing Company, Holland 1969).

Keilis-Borok V.I., Molchan, G.M. and Kronrod, T.L. (1984), Seismic Risk for the Largest Cities of the World, The Geneva papers on risk and Insurance, 9:32, 255-270. Full version: Comput. Seismology, Iss. 16, Moscow (in Russian).

Keilis-Borok, V.I., Molchan, G.M., Gotsadze, O.D., Koridze, A.Ch. and Kronrod, T.L. (1984a). An Attempt of Seismic Risk Estimation for Rural Dwellings in Georgia, Computational seismology, 17, 58-67, Nauka, Moscow (in Russian). Translated in: The Geneva Papers on

risk and Insurance, 1984, Etudes et Dossiers, 77; Natural Disasters and Insurance (IV).

Monachesi, G. and Stucchi, M. (1997), DOM 4.1, an Intensity Data Base of Damaging Earthquakes in the Italian Area.Web site http://emidius.itim.mi.cnr.it/DOM/home.html (GNDT).

Panza, G. F. (1985), Synthetic Seismograms: the Rayleigh Waves Modal Summation, J. Geophys., 58, 125-145.

Panza, G.F. and Suhadolc, P., Complete Strong Motion Synthetics. In Seismic Strong Motion Synthetics (ed. Bolt, B.A.) (Academic Press, Orlando 1987), pp. 153-204.

Panza, G., Craglietto, A. and Suhadolc, P. (1991), Source Geometry of Historical Events Retrieved by Syntethic Isoseismals, Tectonophysics, 193, 173-184.

Panza, G., Cazzaro, R., and Vaccari, F. (1997) Correlation between macroseismic intensities and seismic ground motion parameters, Annali di Geofisica, 40:5, 1371-1382.

Shebalin, N.V. (1959), Determination of Focal Depth from Macroseismic Data with Consideration of the Low Velocity Layer, Problems of Engineering Seismology, Acad. Nauk SSSR, Inst. Fiz. Zemli Trudy, 5(172), 100-113.

Shebalin, N.V. (1972), Macroseismic Data as Information on Source Parameters of Large Earthquakes, Phys. Earth. Planet. Inter., 6, 316-323.

Shebalin, N.V. (2000), Selected Works, vol. 2. (Academy of Mining Sciences, Moscow, *in press*) (in Russian).

Shteinberg, V., Saks, M., Aptikaev, F., Alkaz, V., Gusev, A., Erokhin, L., Zagradnik, I., Kendzera, A., Kogan, L., Lutikov, A., Popova, E., Rautian, T., Chernov, Yu. (1993). Methods of seismic ground motions estimation (Handbook). Seismic ground motions prediction (Engineering seismology problems; Issue 34), Moscow, Nauka, 5-94. (in Russian)

Sirovich, L., Pettenati, F. (1999), Seismotectonic Outline of South-Eastern Sicily: an Evaluation of Available Options for the Earthquake Fault Rupture Scenario, J.Seismology, 3, 213-233.

Tosi, P., De Rubeis, V. and Gasparini, C. (1995), An Analytic Method for Separating Local from

Regional Effects on Macroseismic Intensity, Annali di Geofisica, 38:1, 55-65.

Tosi, P., Tertulliani, A., De Rubeis, V. and Gasparini, C. (1999), Preliminary Results of a Macroseismic Survey of the Colfiorito Sequence (Central Itly), Phys. Chem. Earth (A), 24:6, 477-481.

Trifunac, M.D. and Brady, A.G. (1975), On the Correlation of Seismic Intensity Scales with the Peaks of Recorded Strong Ground Motion, Bull. Seism. Soc. Amer., 65:1, 139-162.

Westaway, R. (1987), The Campania, Southern Italy, Earthquakes of 21 August 1962, Geophys. J. R. Ast. Soc., 88, 1-24.

Zahradnik, J. (1989), Simple method for combines studies of macroseismic intensities and focal mechanisms, Pure Appl. Geophys., 130, 83-97.

FIGURE CAPTIONS.

Figure 1. Number of intensity points per 100 km^2 as a function of the epicentral distance for four Italian earthquakes.

Figure 2. Parameters of the MPF method for the 26.09.1997 Colfiorito earthquake:

(a) radius of smoothing, R;

(b) number of sites, ν, contained in the smoothing circle with radius R.

Bold lines: MPF isolines of *I*=VI and VII.

Figure 3. Illustration of the DB method (for more details see text).

(a) Local Diffused Boundary (LDB) (*shadow* zone) for the data without noise. *Dashed* and *dotted* lines are the axes of the strip;

(b) the same as in (a) for noisy data;

(c) example of Diffused Boundary (DB) of level p=1/3 (*shadow* zone) under the conditions: H=0; the areas A delimited by *bold line*, and B, delimited by *fat line*, contain the noise-free and everywhere dense observations of intensity $\geq I$ and $\leq (I-1)$ respectively; the complementary area to A and B (C plus the shaded area) does not contain intensity data. The local variation of the DB for the case p=1/2 is indicated by the *dashed* curve.

Figure 4. 26.09.1997, M_w=6.0 Colfiorito earthquake:

(a) 40% DB for *I*=VI and *I* =VII (*shaded zones*) and the MPF isolines (*bold*).

Background: IDP map (*point symbols*).

(b) thorny DB for *I* =VI and *I* =VII.

Figure 5. 5.05.1990, Mw=5.8 Potenza earthquake:

(a) the MPF isolines (*bold line*); the *dashed quadrangle* indicated by an arrow delimits a zone of anomalous residuals in *I*: $|\delta I| \geq 2.5$;

Background: IDP map (*point symbols*), NF= "not felt'.

(b) 35% DB (*small squares*) for I in the range from III to VI and aftershocks (*open circles*).

Figure 6. Local spatial variations in the MS data for the 1990 Potenza earthquake:

(a) subdivision of the MS space into elementary areas (cells);

(b-d) histograms for the observed intensity in the cells *b, c, d* of the subdivision in Fig.6a. N is the number of observation sites in each cell.

Figure 7. Reconstruction of noise contaminated synthetic a_p-field (see text for more details), for the 1990 Potenza earthquake, computed in the observation sites:

(a) noise-free isolines of the synthetic a_p-field (*thin lines*) and their reconstruction by the MPF technique (*bold lines*); background: observation sites (*dots*);

(b) thorny DB for I =VI, V, and IV.

Figure 8. 18.10.1936, ML=5.8, Alpago earthquake:

(a) MPF isolines for the MS observations and IDP map (*point symbols*); (A, A′) separates the zone of $I \geq$VI on mountain from that on the plain.

(b) isolines of the synthetic a_p-field (*thin line*) and reconstruction of the theoretical I_a=VI isoline (*bold line*) using the original observation points and the MPF technique.

Figure 9. Secondary parts (*thin line*) of the multi-connected isoseismals for the 11 earthquakes in the zone of Alpago earthquake.

List of the earthquakes (epicenters are shown in the insert): date; area; intensity level, $I+\Delta I$, of each secondary part and its identification in brackets (for ΔI see text: 1) 18.10.1936, Alpago, V+1 (*thick line*; VI-A, VI-B), the area VI-C is an alternative to the area VI-A due to instability of the the polynomial filtering (see text). 2) 29.06.1873, Bellunese, V+1 (2). 3) 7.06.1891, Veronese, IV+1 (3a), V+1 (3b). 4) 27.11.1894, Fransiacorta, IV-1 (4a, *dotted line*), III+1 (4b), II+1 (4c). 5) 4.03.1900, Valdobbiadene, IV+1 (5). 6) 30.10.1901, Salo, IV+1 (6). 7) 27.10.1914, Garfagnana, V+1 (7a), IV+1 (7b). 8) 7.09.1920, Garfagnana,

IV+1 (8). 9) 12.12.1924, Carnia, IV+1 (9). 10) 15.05.1951, Lodigiano, V+1 (10). 11) 15.07.1971, Parmense, IV+1 (11).

Figure 10. 21.08.1962, M_L=6.2 Irpinia earthquake:

(a) MPF isolines for the MS field (*bold*);

(b) 35%–DB for I =VI (*small squares*). The *light small squares* are generated by semi-infinite LDB (the coastline effect).

Background: epicenter (*diamond*), IDP map (*point symbols*).

Figure 11. Isolines of the synthetic a_p-field for the 1962 Irpinia earthquake:

(a) foreshock; (b) main shock; (c) cumulative a_p-effect for the foreshock and mainshock, assumed both with M=6.0.

The source parameters θ, δ, λ, h specify strike, dip, rake, and depth of the source respectively; the *diamond* is the epicenter.

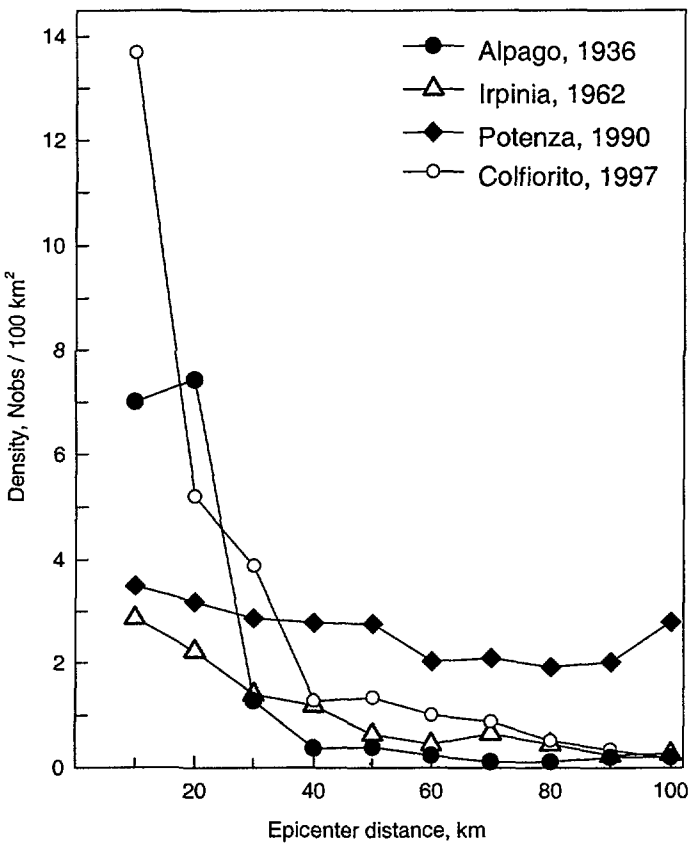
Alpago, 1936
Irpinia, 1962
Potenza, 1990
Colfiorito, 1997
Density, Nobs / 100 km²
Epicenter distance, km
0
2
4
6
8
10
12
14
20
40
60
80
100

Fig. 1

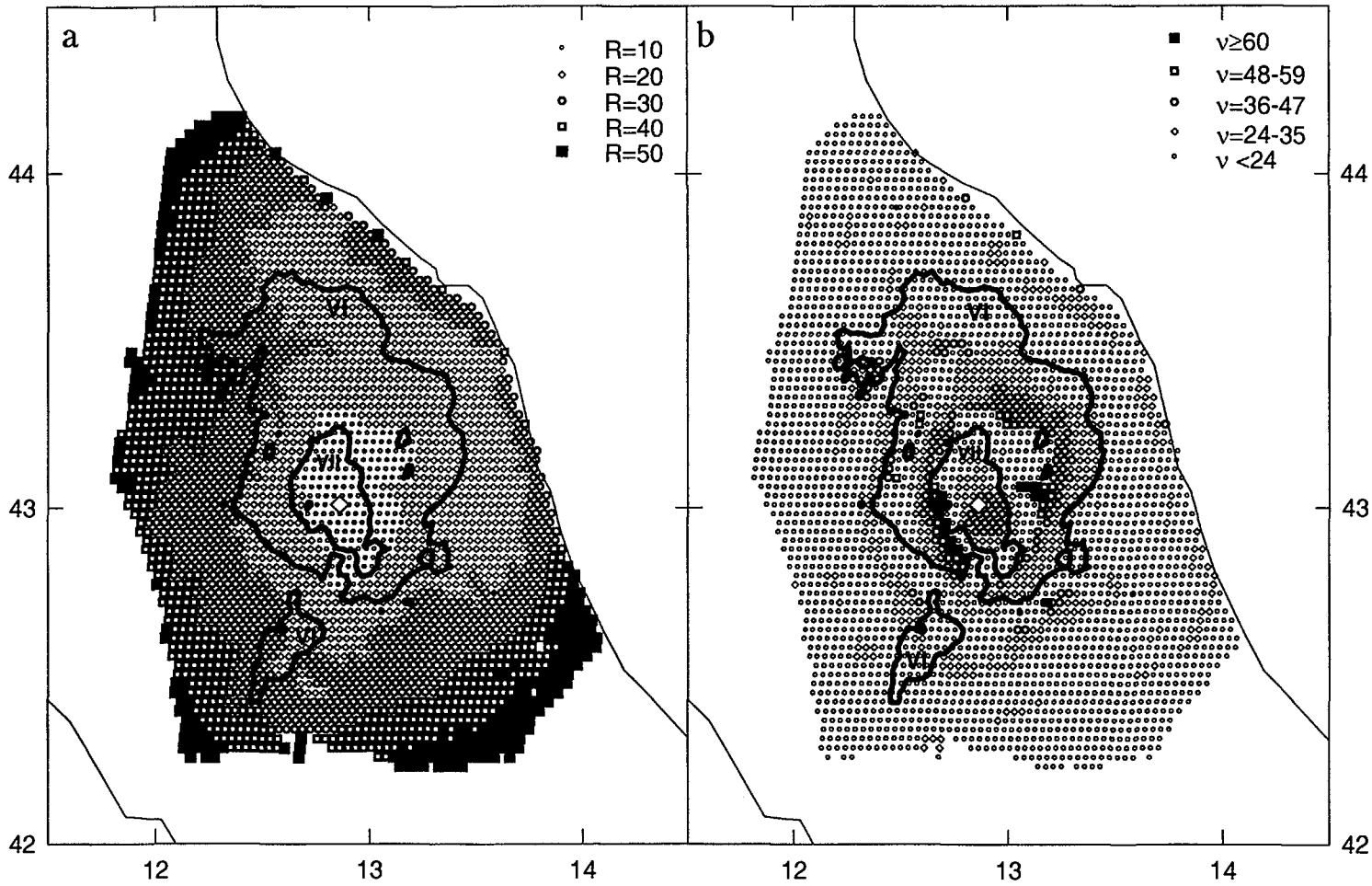
a
R=10
R=20
R=30
R=40
R=50
b
ν≥60
ν=48-59
ν=36-47
ν=24-35
ν <24
44
43
42
12
13
14
VI
VII
VIII
IX

Fig. 2

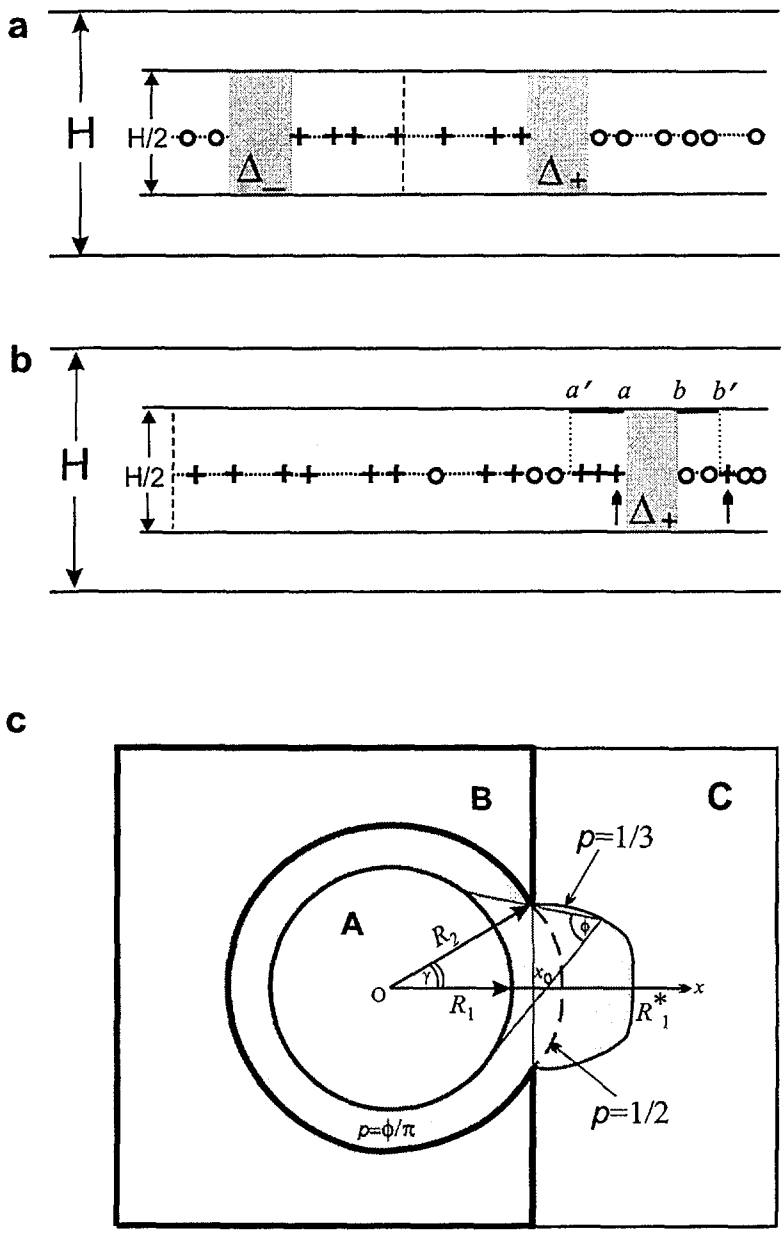

Fig. 3

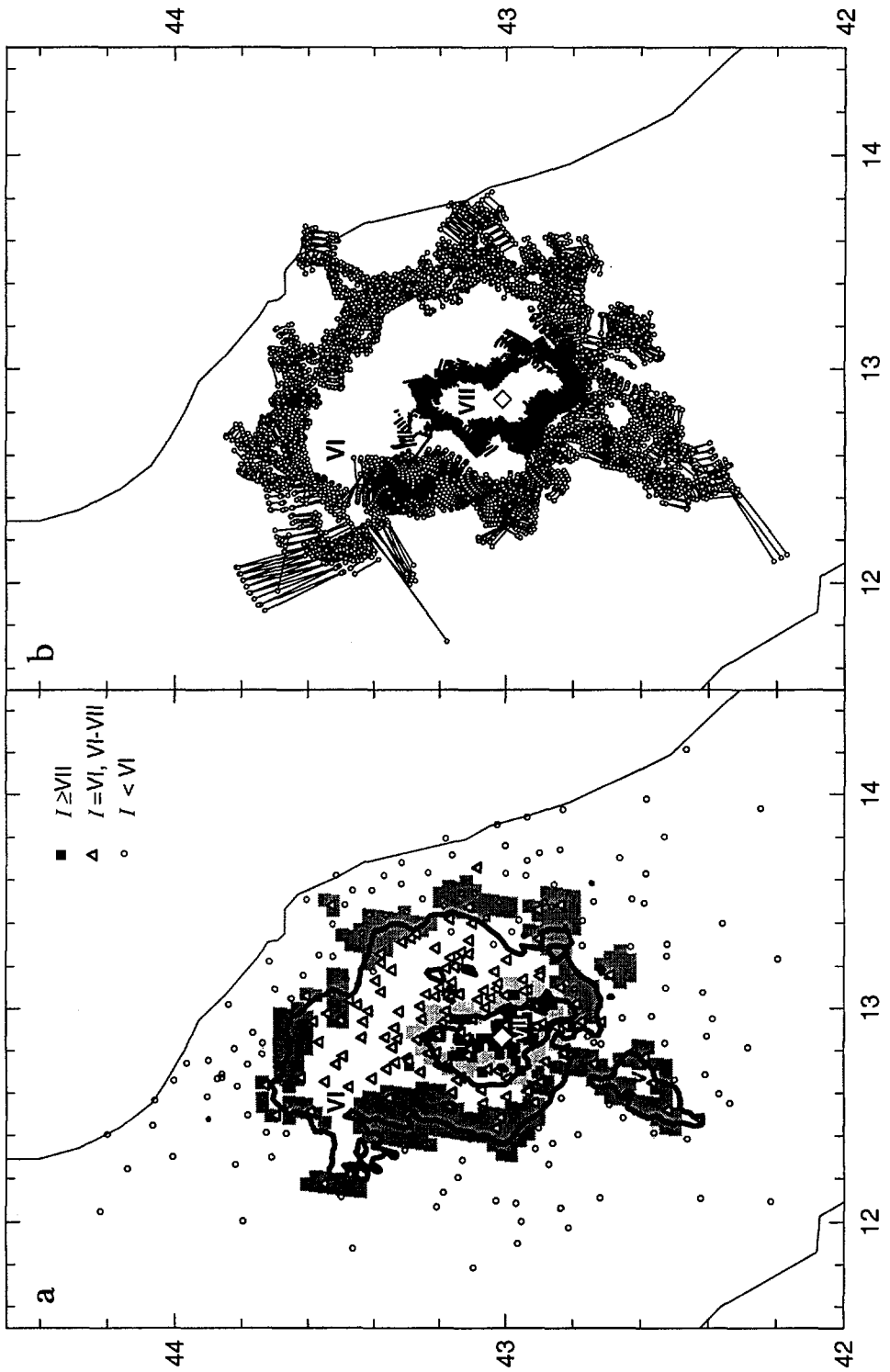

Fig. 4

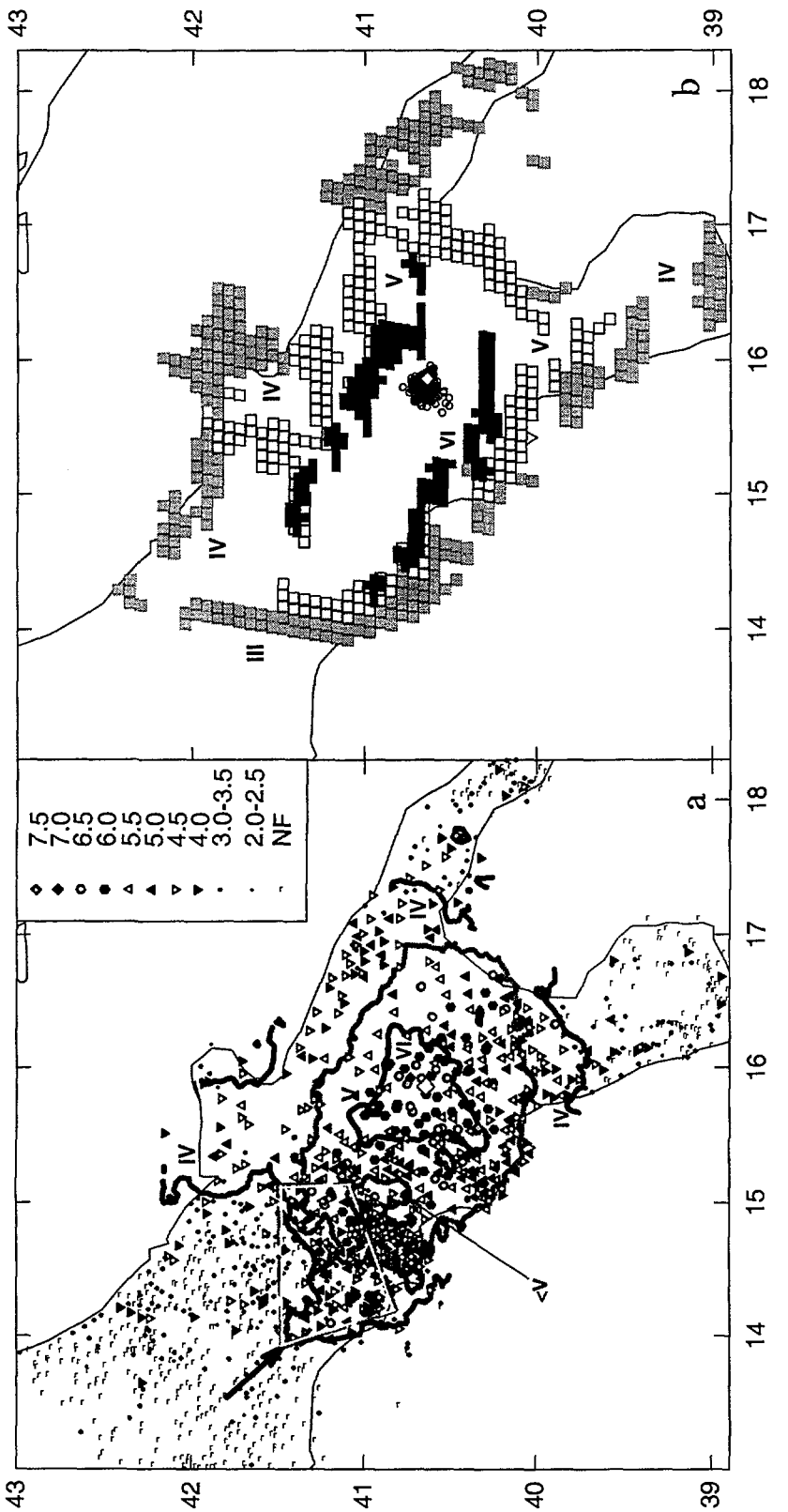
7.5
7.0
6.5
6.0
5.5
5.0
4.5
4.0
3.0-3.5
2.0-2.5
NF
a
b
43
42
41
40
39
14
15
16
17
18
III
IV
V
VI

Fig. 5

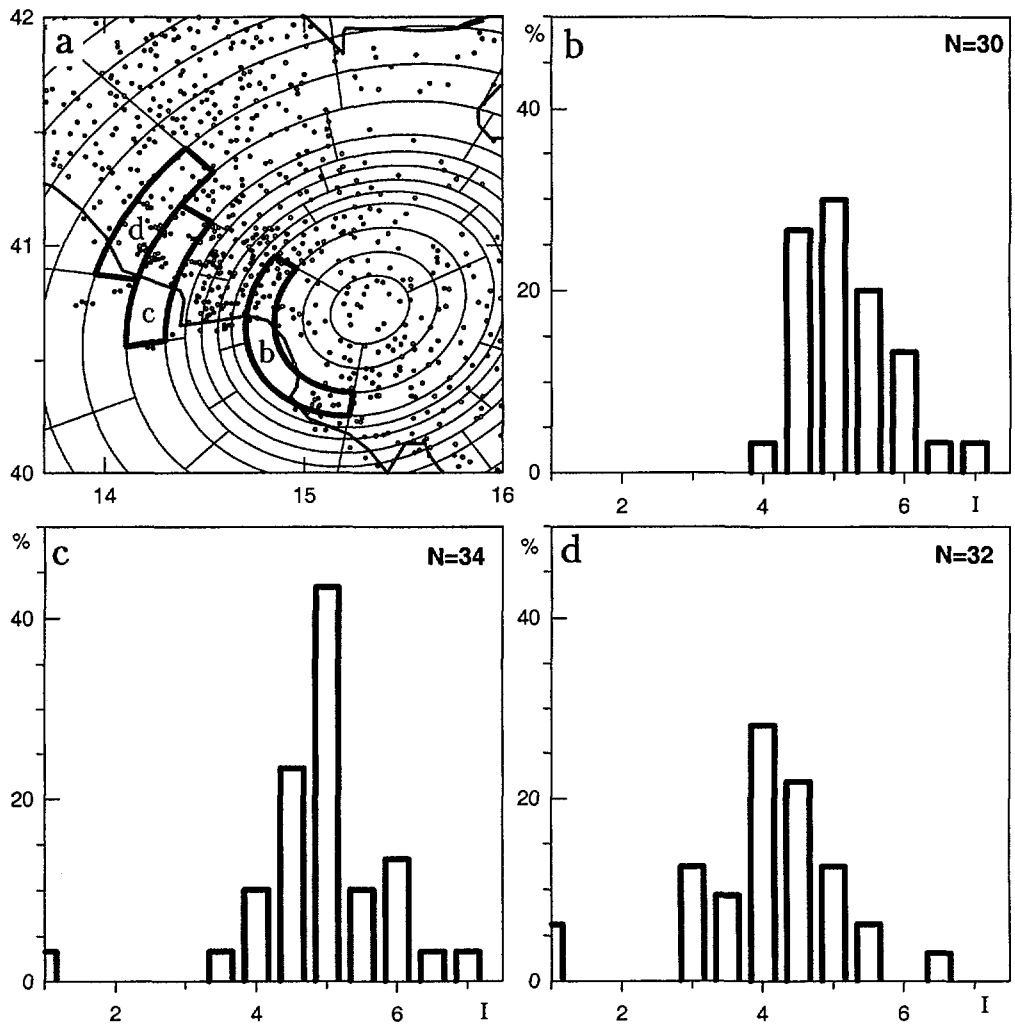

Fig. 6

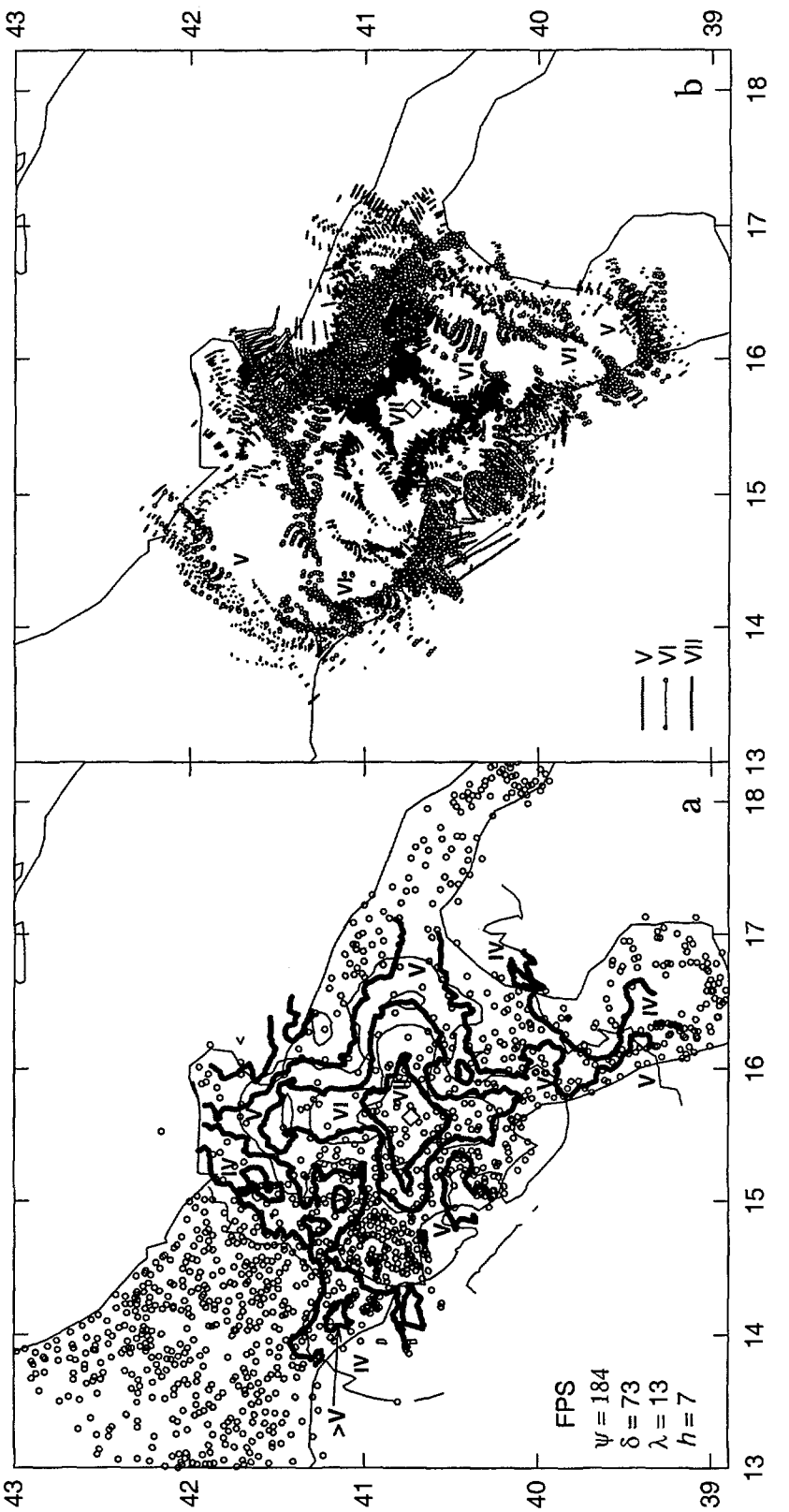

Fig. 7

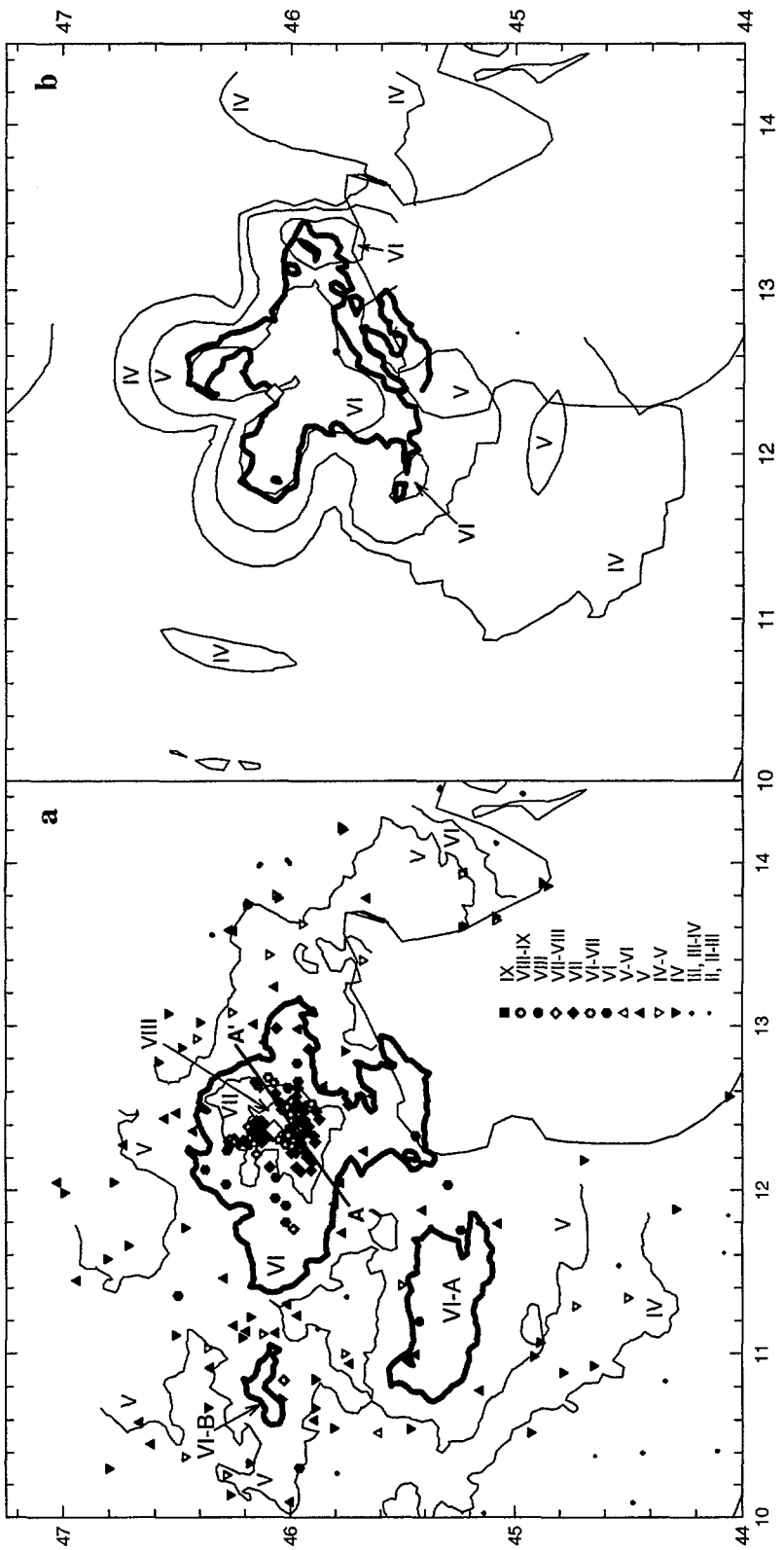
a
b
IX
VIII-IX
VIII
VII-VIII
VII
VI-VII
VI
V-VI
V
IV-V
IV
III, III-IV
II, II-III
VI-B
VI-A
A
A'
B
B'
47
46
45
44
10
11
12
13
14

Fig. 8

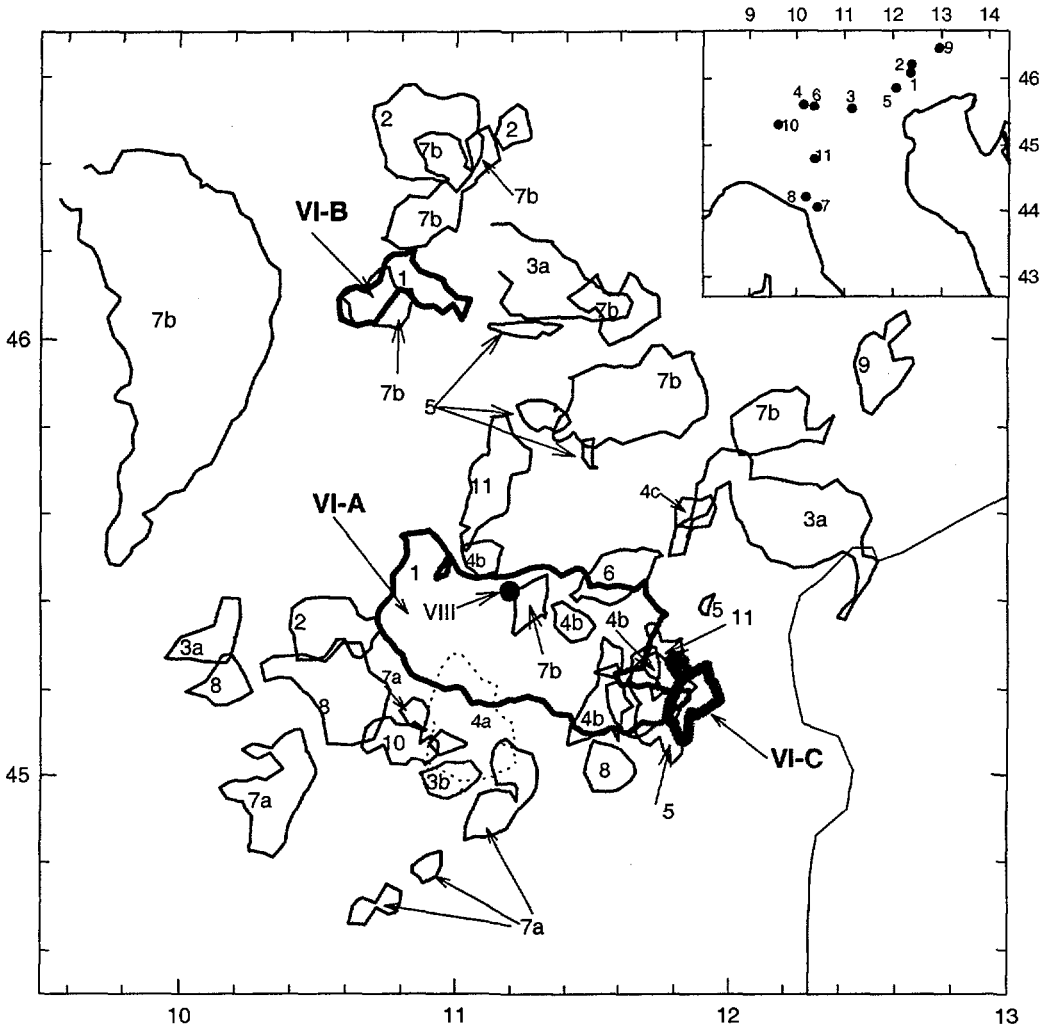
9 10 11 12 13 14
46
45
44
43
VI-B
VI-A
VI-C
VIII
7b
3a
4b
4c
4a
3b
7a
8
10
11
9
6
5
4
3
2
1
46
45
10
11
12
13

Fig. 9

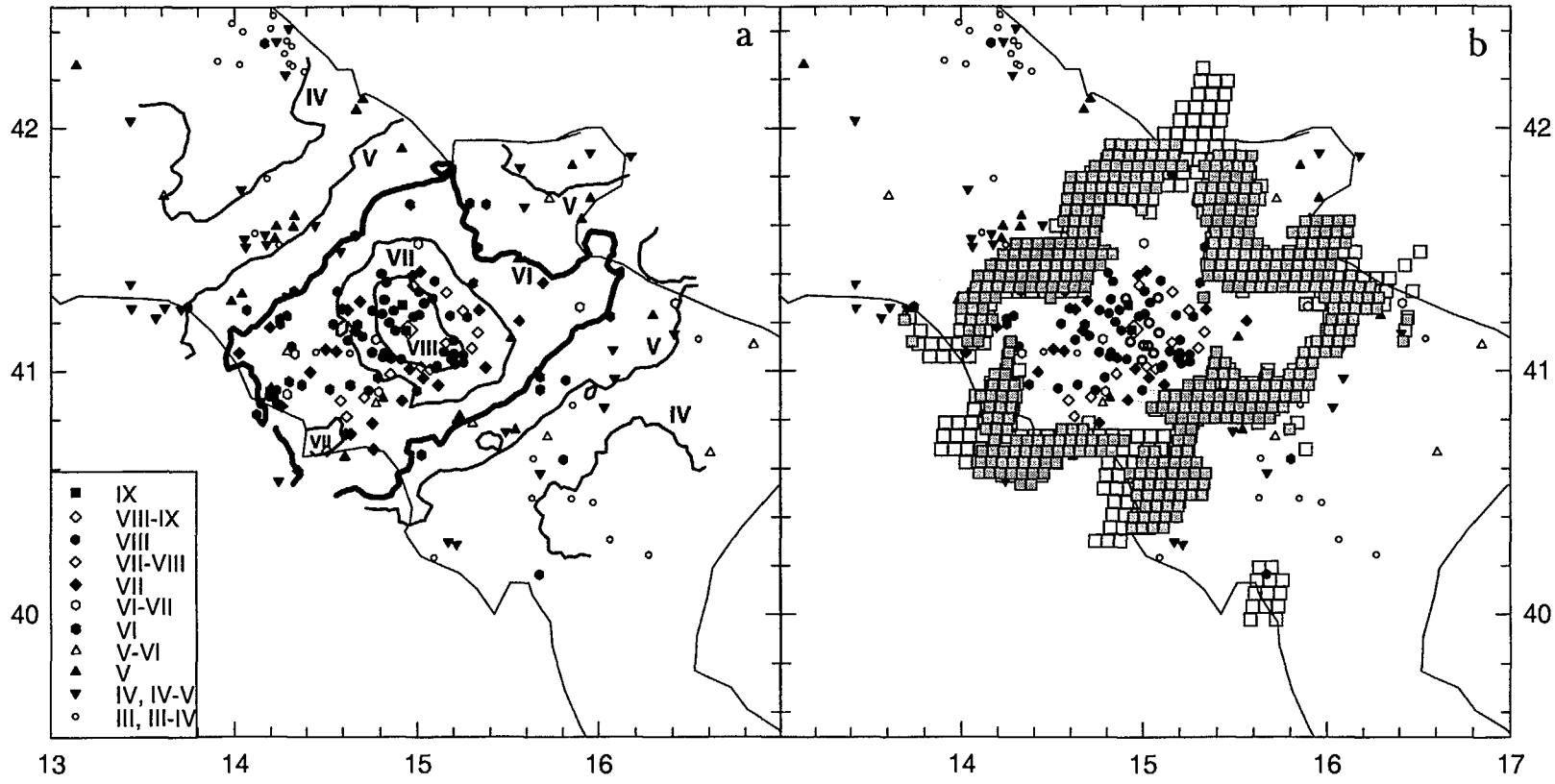
a
b
IX
VIII-IX
VIII
VII-VIII
VII
VI-VII
VI
V-VI
V
IV, IV-V
III, III-IV
42
41
40
13
14
15
16
17

Fig. 10

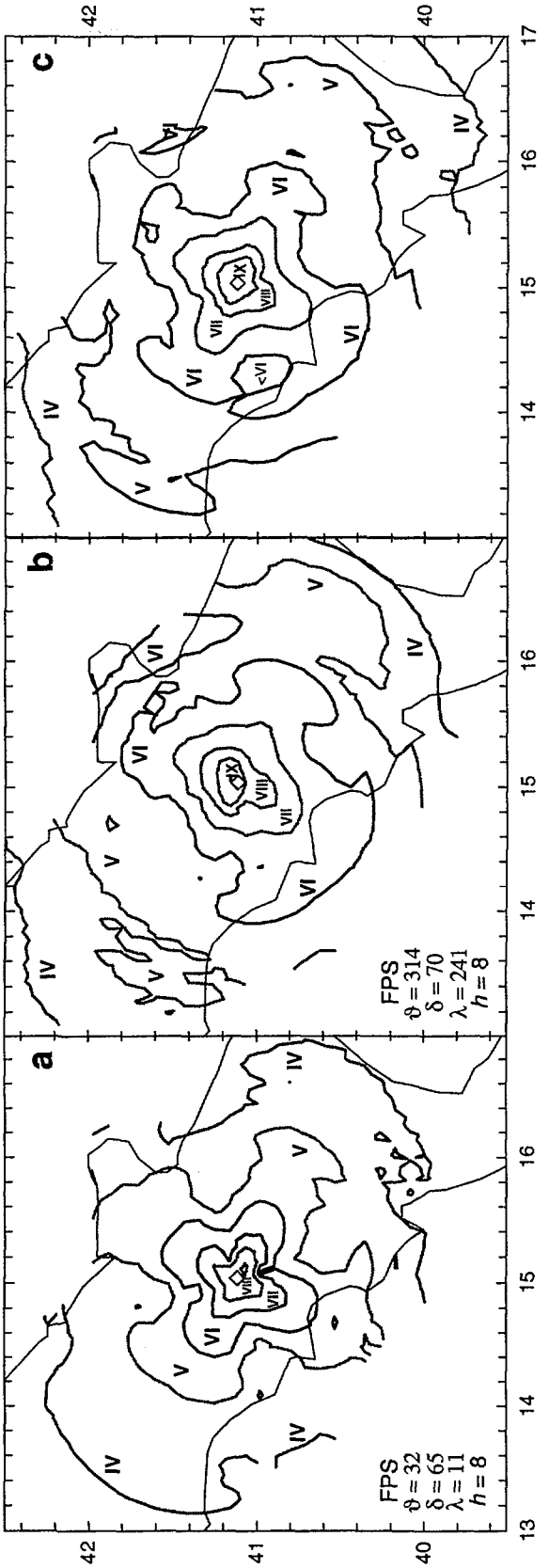
a
b
c
FPS
ϑ = 32
δ = 65
λ = 11
h = 8
FPS
ϑ = 314
δ = 70
λ = 241
h = 8
IV
V
VI
VII
VIII
IX
42
41
40
13
14
15
16
17

Fig. 11